

The selection of variable regions affects effector mechanisms of IgA antibodies against CD20

Mitchell Evers,^{1,*} Thies Rösner,^{2,*} Anna Dünkel,² J. H. Marco Jansen,¹ Niklas Baumann,² Toine ten Broeke,¹ Maaïke Nederend,¹ Klara Eichholz,² Katja Klausz,² Karli Reiding,³ Denis M. Schewe,⁴ Christian Kellner,⁵ Matthias Peipp,² Jeanette H. W. Leusen,¹ and Thomas Valerius^{2,*}

¹Center for Translational Immunology, University Medical Center, Utrecht, The Netherlands; ²Section for Stem Cell Transplantation and Immunotherapy, Department of Medicine II, Christian-Albrechts-University Kiel and University Medical Center Schleswig-Holstein Campus Kiel, Kiel, Germany; ³Biomolecular Mass Spectrometry and Proteomics, Bijvoet Center for Biomolecular Research and Utrecht Institute for Pharmaceutical Sciences, University of Utrecht, and Netherlands Proteomics Center, Utrecht, The Netherlands; ⁴Pediatric Hematology/Oncology, Acute Lymphoblastic Leukemia–Berlin-Frankfurt-Münster Study Group, Christian-Albrechts-Universität and University Medical Center Schleswig-Holstein Campus Kiel, Kiel, Germany; and ⁵Department of Transfusion Medicine, Cell Therapeutics and Hemostaseology, University Hospital, LMU Munich, Munich, Germany

Key Points

- Variable regions of CD20 IgA antibodies affected effector mechanisms and efficacy in vitro and in vivo.
- Disruption of CD47-SIRP α interactions improved ADCP and ADCC by CD20 IgA antibodies.

Blockade of the CD47-SIRP α axis improves lymphoma cell killing by myeloid effector cells, which is an important effector mechanism for CD20 antibodies in vivo. The approved CD20 antibodies rituximab, ofatumumab, and obinutuzumab are of human immunoglobulin G1 (IgG1) isotype. We investigated the impact of the variable regions of these 3 CD20 antibodies when expressed as human IgA2 isotype variants. All 3 IgA2 antibodies mediated antibody-dependent cellular phagocytosis (ADCP) by macrophages and antibody-dependent cellular cytotoxicity (ADCC) by polymorphonuclear cells. Both effector mechanisms were significantly enhanced in the presence of a CD47-blocking antibody or by glutaminyl cyclase inhibition to interfere with CD47-SIRP α interactions. Interestingly, an IgA2 variant of obinutuzumab (OBI-IgA2) was consistently more potent than an IgA2 variant of rituximab (RTX-IgA2) or an IgA2 variant of ofatumumab (OFA-IgA2) in triggering ADCC. Furthermore, we observed more effective direct tumor cell killing by OBI-IgA2 compared with RTX-IgA2 and OFA-IgA2, which was caspase independent and required a functional cytoskeleton. IgA2 variants of all 3 antibodies triggered complement-dependent cytotoxicity, with OBI-IgA2 being less effective than RTX-IgA2 and OFA-IgA2. When we investigated the therapeutic efficacy of the CD20 IgA2 antibodies in different in vivo models, OBI-IgA2 was therapeutically more effective than RTX-IgA2 or OFA-IgA2. In vivo efficacy required the presence of a functional IgA receptor on effector cells and was independent of complement activation or direct lymphoma cell killing. These data characterize the functional activities of human IgA2 antibodies against CD20, which were affected by the selection of the respective variable regions. OBI-IgA2 proved particularly effective in vitro and in vivo, which may be relevant in the context of CD47-SIRP α blockade.

Submitted 26 February 2021; accepted 5 July 2021; prepublished online on *Blood Advances* First Edition 15 September 2021; final version published online published online 4 October 2021. DOI 10.1182/bloodadvances.2021004598.

*M.E. and T.R. contributed equally to this work.

Data sharing requests should be sent to Thies Rösner (thies.roesner@uksh.de), Mitchell Evers (j.g.m.evers-8@umcutrecht.nl), or Thomas Valerius (t.valerius@med2.uni-kiel.de).

The full-text version of this article contains a data supplement.

© 2021 by The American Society of Hematology

Introduction

Myeloid cells often constitute a relevant population of the tumor immune cell infiltrate,¹ where their presence is commonly associated with a poor prognosis for patients.² On the other hand, macrophages were identified as the predominant effector cell population for the CD20 antibody rituximab (RTX) in mice.^{3,4} Several approaches have been identified to improve the tumor cell-killing capacity of myeloid cells, including Fc engineering of tumor-directed antibodies⁵ and blockade of myeloid checkpoint molecules.⁶ Among the latter, blockade of CD47-SIRP α interactions by the CD47 antibody Hu5F9-G4 (magrolimab) is currently the most advanced in clinical development.⁷ CD47 is a broadly expressed transmembrane protein that provides a “don’t eat me signal” to phagocytes by binding to the α - isoform of the signaling inhibitory receptor protein (SIRP α ; CD172a). SIRP α binding triggers immunoreceptor tyrosine-based inhibitory motif-dependent signaling in phagocytes and, thereby, inhibits their phagocytic and tumor cell killing activity.⁸ Blockade of CD47-SIRP α interactions has been demonstrated to enhance the therapeutic activity of several tumor-directed antibodies in preclinical models.^{9,10} Recently, Advani et al were the first to report on a phase 1 clinical study in which the CD47 antibody magrolimab was combined with RTX in lymphoma patients who had relapsed after or were refractory to RTX. Importantly, impressive clinical response rates were observed in heavily pretreated patients with diffuse large B-cell lymphoma (DLBCL) or follicular lymphoma.¹¹

All currently approved and clinically developed CD20 antibodies are of the human immunoglobulin G1 (IgG1) isotype, because IgG1 effectively recruits natural killer (NK) cells for antibody-dependent cellular cytotoxicity (ADCC), triggers antibody-dependent phagocytosis (ADCP) by macrophages, activates complement via the classical pathway, and has a long serum half-life by binding to FcRn. However, human IgG1 is suboptimal for the induction of tumor cell killing by human polymorphonuclear cells (PMNs), the most numerous myeloid effector cell population in blood.^{12,13} Several studies have shown that PMN-mediated tumor cell killing is triggered more effectively by human IgA antibodies carrying the same variable regions than by their parental IgG1 antibodies.¹⁴⁻¹⁹ Human IgA antibodies have not been evaluated clinically, but progress has been made in developing IgA molecules with improved biopharmaceutical and pharmacokinetic properties.²⁰

CD20 antibodies can be classified according to their ability to segregate CD20 in lipid rafts as type I (lipid raft formation) or type II (no lipid raft formation).²¹ CD20 antibodies can mediate direct cell killing, lymphoma cell phagocytosis by macrophages, trogocytosis by PMNs, and ADCC by NK cells; Fc receptor-mediated functions are enhanced for obinutuzumab (OBI) compared with RTX, presumably as a result of its glycoengineered Fc portion.²²⁻²⁴ However, CD20 antibodies of the human IgG1 isotype did not trigger ADCC by human PMN, whereas IgA2 variants with the same variable regions proved effective.^{13,15} To understand whether CD47-SIRP α blockade could overcome IgG1’s inefficacy in triggering ADCC by PMNs, we tested RTX, ofatumumab (OFA), and OBI in the absence or presence of CD47 blockade. In addition, we generated IgA2 variants of these 3 CD20 antibodies (RTX-IgA2, OBI-IgA2, and OFA-IgA2) and investigated their modes of lymphoma cell killing in detail. Interestingly, OBI-IgA2 was more effective than RTX-IgA2 and OFA-IgA2 *in vitro* and *in vivo*, indicating that the variable regions of IgA CD20 antibodies can

critically determine their therapeutic efficacy. To the best of our knowledge, differences in effector cell recruitment that depend on the variable regions have not been described for CD20 antibodies and may prove relevant in the context of myeloid checkpoint blockade.

Materials and methods

Experiments with human material were approved by the Ethical Committees of the participating institutions in accordance with the Declaration of Helsinki. Healthy volunteers and patients gave written informed consent before analyses.

Cell lines and primary patient samples

Cell lines were obtained from the German Collection of Microorganisms and Cell Cultures (Braunschweig, Germany) or from the American Type Culture Collection (Manassas, VA). Generation of human CD20-transgenic (Tg) CHO-K1 cells was described previously.¹⁵ EL4 cells stably transduced with human CD20 were described previously.^{25,26} All cells were grown in media, as recommended by the suppliers, and were obtained between 2011 and 2016. Primary tumor cell samples from patients with Waldenström disease or chronic lymphocytic leukemia (CLL) were prepared from peripheral blood by density gradient centrifugation using Ficoll (GE Healthcare, Chicago, IL).

Antibodies

The approved CD20 antibodies RTX (human IgG1; 2B8; Rituxan) and OBI (afucosylated human IgG1; GA101; GAZYVA) were from Roche (Basel, Switzerland). Ofatumumab (human IgG1; 2F2; Arzerra) was obtained from Novartis (Basel, Switzerland). The EGFR antibody cetuximab (human IgG1, 225; Erbitux) and the C5 antibody eculizumab (human IgG2/IgG4 chimera; 5G1.1; SOLIRIS) were purchased from Merck (Kenilworth, NJ) and Alexion (New Haven, CT), respectively. For murine antibodies and newly generated antibody variants see supplemental Materials and methods.

Direct Fab-mediated cell death analyses

To analyze direct Fab-mediated cell death of lymphoma cells, 1.4×10^5 target cells were incubated with CD20 or isotype control antibodies (all at 10 μ g/mL) at 37°C and 5% CO₂, in the presence or absence of 10 μ M Latrunculin B (LatB; Cayman Chemical Company, Ann Arbor, MI) or 50 μ M carbobenzoxy-valyl-alanyl-aspartyl-[O-methyl]-fluoromethylketon (Z-VAD-FMK; APEXIO Technology, Houston, TX). Photographs were taken 24 hours later using an Axiovert 40C microscope and an AxioCam ERc 5s camera (both from Zeiss, Oberkochen, Germany). Next, cells were stained using an FITC Annexin V Apoptosis Detection Kit + 7-aminoactinomycin (Bio Legend, San Diego, CA), according to the manufacturer’s instructions, and analyzed by flow cytometry using a Navios flow cytometer, Brea, Beckman Coulter, CA). To quantify lysosomal cell death or apoptosis, 1×10^5 target cells were incubated with CD20 antibodies (10 μ g/mL) at 37°C and 5% CO₂. After 5 hours of incubation, LysoTracker Red (50 nM; Invitrogen, Carlsbad, CA) was added for 1 hour to determine lysosomal cell death or cells were treated after 6 hours with 10 nM DiOC6 and 20 nM TO-PRO-3 (both from Thermo Fisher, Waltham, MA), following the manufacturer’s instructions. Afterward, cells were analyzed by flow cytometry (BD LSRFortessa; BD Biosciences, Franklin Lakes, NJ). Triton solubility of lipid rafts was determined as described previously.²¹

Complement binding and deposition

Complement component binding and deposition were characterized by indirect flow cytometry. Target cells (2.5×10^5) were incubated with isotype control or with the indicated CD20 antibodies (all at 10 $\mu\text{g}/\text{mL}$) for 15 minutes at 4°C. Subsequently, a 25% volume-to-volume ratio of human serum was added as a source of complement in the presence of the C5-blocking antibody eculizumab (100 $\mu\text{g}/\text{mL}$) to avoid complement-dependent cytotoxicity (CDC). Samples were stained with polyclonal FITC-conjugated C1q, C4b/c, or C3b/c antibodies (all from Agilent, Santa Clara, CA) and analyzed on a flow cytometer (Navios; Beckman Coulter).

CDC assays

CDC assays were performed as described previously.¹⁵ Briefly, target cells were labeled with 200 μCi [⁵¹Cr] for 2 hours. A 25% volume-to-volume ratio of freshly drawn human serum was used as a source of complement in the presence of the indicated antibodies (0-50 $\mu\text{g}/\text{mL}$). The percentage of [⁵¹Cr] release was calculated using the formula: percentage lysis = (experimental cpm – basal cpm)/(maximal cpm – basal cpm) \times 100; maximal [⁵¹Cr] release was determined by adding Triton-X (2% final concentration) to target cells, and basal release was measured in the absence of sensitizing antibodies.

Isolation of human effector cells

Human effector cells were isolated from peripheral blood (PMNs) of healthy volunteers or were generated from leukoreduction system chambers (macrophages) from blood donors, using PolymorphoPrep (PROGEN, Heidelberg, Germany) or Ficoll (GE Healthcare), as previously described.¹² In brief, monocyte-derived macrophages were generated using monocyte-attachment medium (PromoCell, Heidelberg, Germany), according to the manufacturer's instructions. For macrophage generation, 50 ng/mL macrophage colony-stimulating factor (PeproTech, Rocky Hill, NJ) was added for ≥ 7 days.

ADCC assays

Analysis of ADCC was performed using [⁵¹Cr] release assays, as described previously.²⁷ granulocyte-macrophage colony-stimulating factor (50 U/mL; CellGenix, Freiburg, Germany)–stimulated PMNs, antibodies at various concentrations, and medium were added to round-bottom microtiter plates (Nunc, Rochester, NY). Assays were started by the addition of effector and target cells at the indicated E:T ratios. After 3 h at 37°C, [⁵¹Cr] release from triplicate samples was measured. The percentage of cellular cytotoxicity was calculated using the same formula as for CDC assays.

ADCP assays

ADCP experiments were performed as described.²⁸ In brief, lymphoma cells were washed in phosphate buffered saline (PBS) and labeled with 7.5 μM carboxyfluorescein succinimidyl ester (BioLegend, San Diego, CA). Twenty thousand macrophages were seeded per well in μ -slide 8-well chambered coverslips (ibidi, Gräfelfing, Germany) and allowed to adhere overnight. Forty thousand carboxyfluorescein succinimidyl ester–labeled tumor cells were added. Antibodies were applied at a final concentration of 10 $\mu\text{g}/\text{mL}$. Cells were incubated for 2 hours at 37°C. ADCP was determined by fluorescence microscopy (Nikon, Tokyo, Japan). ADCP was calculated as phagocytic index using the formula: ADCP [phagocytic index] = (number of engulfed target cells/number of macrophages) \times 100.

In vivo experiments

All experiments were performed in accordance with international guidelines and approved by the national Central Authority for Scientific Procedures on Animals and the local experimental animal welfare body (AVD115002016410). A detailed description is available in supplemental Materials and methods.

Data processing and statistical analyses

Data were generated from ≥ 3 independent experiments using blood from different healthy donors. Graphical and statistical analyses were performed using GraphPad Prism 5.0 or 8.0 (GraphPad Software, San Diego, CA). Group data are reported as mean \pm standard error of the mean (SEM) or standard deviation; half-maximal effective concentrations were calculated from dose-response curves and also reported as mean \pm SEM. Significance was determined by 1- or 2-way analysis of variance (ANOVA) repeated-measures test with the Bonferroni post hoc correction.

Results

Blockade of CD47-SIRP α interactions improves CD20 IgG1 antibody-mediated ADCP by macrophages but does not trigger ADCC by PMNs

First, we investigated myeloid effector cell recruitment by the 3 clinically approved CD20 antibodies RTX, OFA, and OBI in the presence or absence of CD47-SIRP α inhibition. To disrupt CD47-SIRP α interaction, assays were performed using an Fc silent IgG2 α variant of the CD47 antibody 5F9 (Figure 1) or by treating target cells with a glutaminyl cyclase inhibitor, SEN177 (supplemental Figure 1A). Recent results by Logtenberg et al²⁹ demonstrated that SEN177 inhibited a functionally important posttranslational modification of CD47 (pyroglutamate formation) and, thereby, impaired SIRP α binding. As expected, all 3 CD20 antibodies mediated ADCP by macrophages, which was significantly improved by CD47-SIRP α inhibition for a mantle cell lymphoma cell line (Mino) and a Burkitt lymphoma cell line (Raji) (Figure 1A; supplemental Figure 1B). Next, we used neutrophils in ADCC assays with the same 3 CD20 antibodies. As expected from previous studies,^{13,15,30} none of them triggered ADCC by PMNs (Figure 1B; supplemental Figure 1C). Interestingly, this inefficacy of CD20 IgG1 antibodies in PMN-mediated ADCC could not be overcome by disruption of CD47-SIRP α interactions, as demonstrated (Figure 1B; supplemental Figure 1C). Together, these results demonstrate that CD47 blockade cannot overcome the previously reported inefficacy of CD20 antibodies of the human IgG1 isotype to recruit PMNs for ADCC against lymphoma cells.

Blockade of the CD47-SIRP α axis improves myeloid effector cell recruitment of the IgA2 isotype by CD20 antibodies

Because CD20 antibodies of the IgG1 isotype did not use neutrophils for ADCC, we generated IgA2.0 isotype switch variants of the 3 approved CD20 antibodies: RTX, OFA, and OBI. These IgA antibodies displayed the expected biochemical properties and binding to CD20 (supplemental Figure 2). Similar to IgG1, CD20 antibodies of the IgA2 isotype also induced macrophage-mediated ADCP of lymphoma cells, which was significantly enhanced by CD47 blockade (Figure 2A), as well as by glutaminyl cyclase inhibition (supplemental

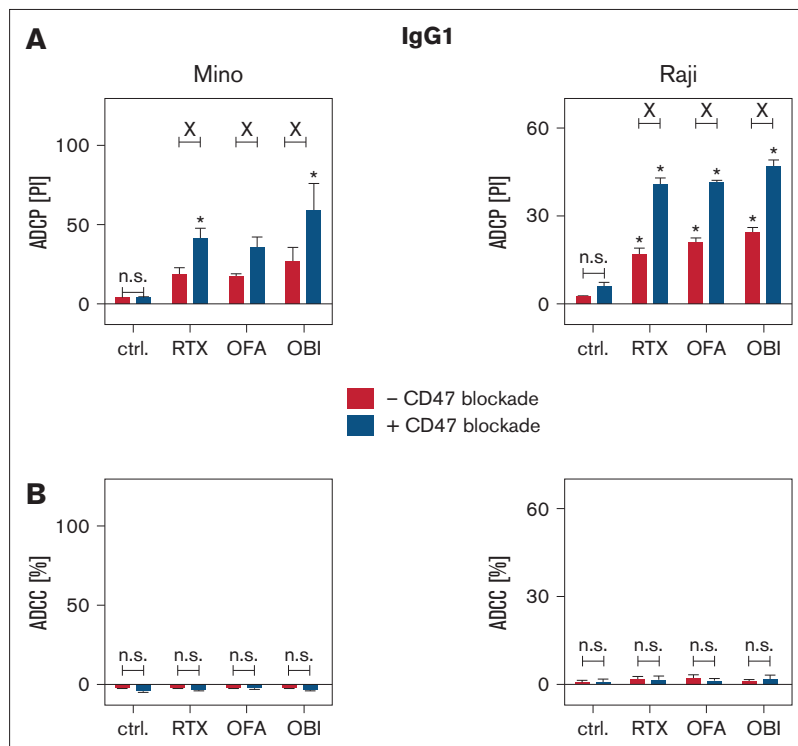


Figure 1. Blockade of CD47-SIRP α interactions improves CD20 IgG1 antibody-mediated ADCP by macrophages but does not trigger ADCC by PMNs. Macrophage-mediated ADCP was assessed by fluorescence microscopy (A), whereas ADCC by PMNs was investigated in 3-hour [^{51}Cr] release assays (B). An IgG2 α version of the CD47 antibody 5F9 (10 $\mu\text{g}/\text{mL}$) was used to block CD47-SIRP α interactions. Mino (mantle cell lymphoma) and Raji (Burkitt lymphoma) cells served as target cells (left and right panels, respectively). The CD20 antibody RTX, OFA, or OBI was used at 10 $\mu\text{g}/\text{mL}$; E:T ratios were 80:1 in ADCC assays and 1:2 in ADCP assays. Results are mean \pm SEM from ≥ 3 experiments with effector cells from different donors. *Significant ADCP by CD20 antibodies vs control (ctrl.) antibody. XSignificant differences in the absence or presence of CD47 blockade. Significant differences ($P < .05$) were calculated using ANOVA. n.s., not significant; PI, phagocytic index.

Figure 3A). Against lymphoma cell lines that are difficult to kill for PMNs, such as Mino and Raji, CD20 IgA2 antibodies alone triggered low levels of ADCC (Figure 2B). However, PMN-mediated ADCC was significantly enhanced for all 3 CD20 IgA2 antibodies in the presence of a CD47-blocking antibody (Figure 2B) or by glutaminy cyclase inhibition (supplemental Figure 3B).

When more susceptible DLBCL lymphoma cells (SU-DHL-4) served as targets in PMN-mediated ADCC assays, IgA2 variants of all 3 CD20 antibodies alone triggered significant ADCC by PMNs in an antibody concentration-dependent manner or at different E:T ratios (Figure 2C). Interestingly, OBI-IgA2 was significantly more effective than RTX-IgA2 or OFA-IgA2 in both ADCC setups. Thus, we investigated whether this also held true for other B-cell lines and primary lymphoma cells.

OBI-IgA2 is more effective than RTX-IgA2 at triggering ADCC by PMNs

The glycoengineered CD20 antibody OBI is known to trigger improved ADCC by NK cells compared with other CD20 antibodies, which is explained by its enhanced Fc γ R11a binding on NK cells due to its lower level of Fc fucosylation.³¹ Unexpectedly, OBI-IgA2 also appeared to be more effective than RTX-IgA2 in triggering ADCC by PMNs. This observation cannot be explained by differences in fucosylation, because the glycosylation profiles of all 3 CD20 IgA antibodies were similar (supplemental Figure 2C), and glycosylation of

IgA was demonstrated not to contribute to Fc α RI (CD89) binding.³² Next, we compared PMN-mediated ADCC by OBI-IgA2 vs RTX-IgA2 against a broader panel of CD20⁺ lymphoma cell lines, reflecting different biological entities of B-cell lymphomas. As demonstrated, OBI-IgA2 triggered significant ADCC by PMNs against all tested cell lines and was often significantly more potent than the respective RTX-IgA2 variant (Figure 3A). Importantly, OBI-IgA2 also triggered significant ADCC by PMNs against isolated primary lymphoma cells from patients with Waldenström disease or CLL, as well as against isolated primary leukemia cells from patients with CLL (Figure 3B). Here, OBI-IgA2 was significantly more potent than the respective approved CD20 antibody of the IgG1 isotype.

Complement activation by CD20 antibodies of the IgA2 isotype

Another well-documented effector mechanism of type I CD20 antibodies (eg, RTX and OFA) is CDC,^{33,34} whereas the CDC activity of type II antibodies (eg, OBI) is considerably weaker.³⁵ Interestingly, IgA antibodies against CD20 also demonstrated C1q-dependent CDC activity,^{15,36} although IgA lacks a C1q binding site.³⁷ Thus, we compared complement activation between the approved IgG1 CD20 antibodies and our novel IgA2 variants. As expected, all 3 IgG1 antibodies mediated significant CDC, with OBI being significantly less effective than the type I antibodies RTX and OFA ($P < .05$; Figure 4A, left panel). Interestingly, the 3 IgA2

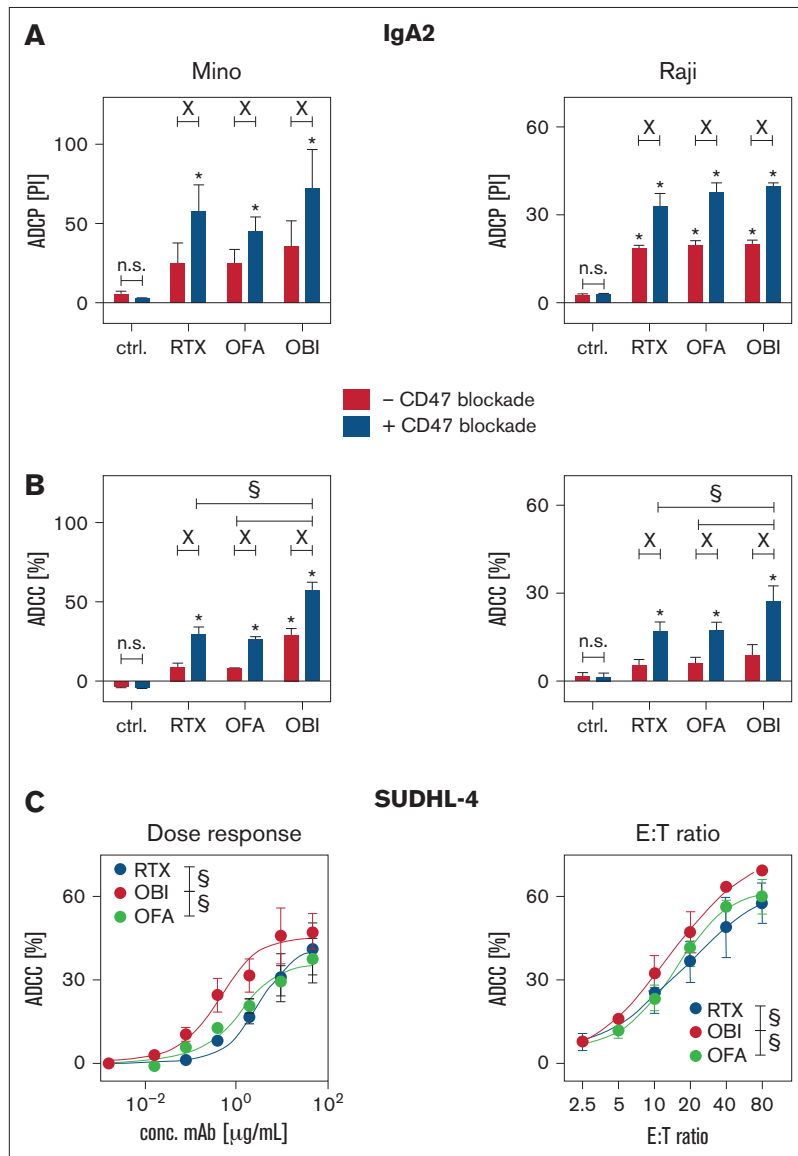


Figure 2. Blockade of the CD47-SIRP α axis improves myeloid effector cell recruitment by CD20 antibodies of the IgA2 isotype. Macrophage-mediated ADCC by CD20 antibodies of the IgA2 isotype was determined by fluorescence microscopy (A), whereas ADCC by PMNs was investigated in 3-hour [⁵¹Cr] release assays (B). An IgG2 α version of the CD47 antibody 5F9 (10 μ g/mL) was used to block CD47-SIRP α interactions. The CD20 antibodies RTX, OFA, and OBI were used at 10 μ g/mL; E:T ratios were 80:1 in ADCC assays and 1:2 in ADCC assays. (C) Increasing concentrations of IgA2 variants of RTX, OFA, and OBI (left panel) or increasing E:T ratios (right panel) were compared in 3-hour [⁵¹Cr] release ADCC assays using PMNs as effector cells. Target cells were Mino cells (mantle cell lymphoma) and Raji cells (Burkitt lymphoma) (left and right panels, respectively) in (A) and (B) and SU-DHL-4 cells (DLBCL) in (C). CD20 antibodies are depicted as colored circles. Results are mean \pm SEM from \geq 3 experiments with effector cells from different donors. *Significant difference vs control (ctrl.) antibody. ^xSignificant difference in the absence and presence of CD47 blockade. ^sSignificant difference between OBI-IgA2 and RTX-IgA2 or OFA-IgA2. Significant differences ($P < .05$) were calculated using ANOVA. conc., concentration; mAb, monoclonal antibody; n.s., not significant.

molecules also triggered CDC with OBI-IgA2 being significantly less efficient than RTX-IgA2 and OFA-IgA2 ($P < .05$, ANOVA; Figure 4 A, right panel). Maximal CDC by all 3 IgA2 variants was significantly lower compared with the respective IgG1 molecules (Figure 4B).

To better understand CDC triggered by IgA antibodies against CD20, complement binding (C1q) and deposition (C4b/c and C3b/c) on lymphoma cells was measured by flow cytometry (Figure 4C). For CD20 antibodies of the IgG1 isotype, the expected differences in C1q binding efficacy were observed (OFA > RTX > OBI). None

of the 3 IgA2 antibodies triggered measurable C1q binding. All 3 IgG1 antibodies showed high levels of C4b/c deposition, whereas C4b/c deposition by IgA2 antibodies was low, but detectable. All antibodies deposited C3b/c on lymphoma cells, indicative of effective C5 convertase formation. All IgA2 variants were significantly less effective than were the respective IgG1 molecules in C4b/c and C3b/c deposition (Figure 4C). Together, these results demonstrate that IgG and IgA antibodies perform CDC in vitro. IgG1 antibodies do this more efficiently; OBI is the least efficient in CDC induction, as IgG1 and IgA2 variants.

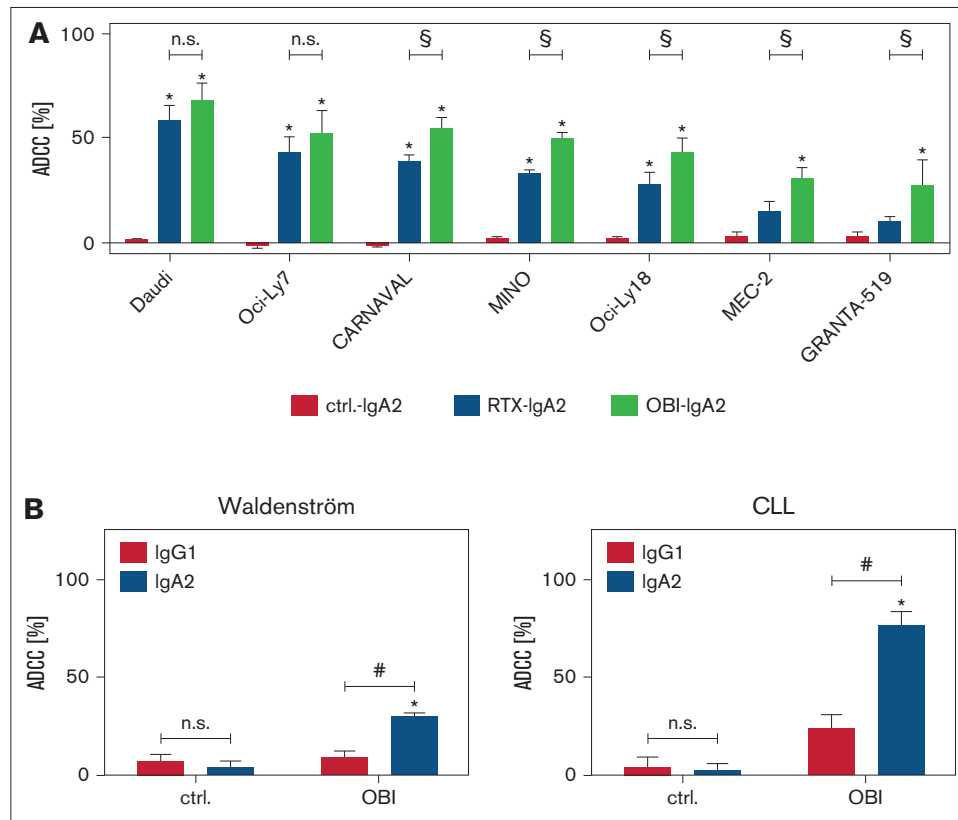


Figure 3. OBI-IgA2 is more effective than RTX-IgA2 at triggering ADCC by PMNs. (A) Cell lines representing different B-cell lymphoma entities (Daudi (Burkitt lymphoma); Oci-Ly7, CARNAVAL, and Oci-Ly18 (DLBCL); GRANTA-519 and MINO (mantle cell lymphoma); MEC-2 (CLL)) served as target cells in [⁵¹Cr] release assays. (B) ADCC was investigated in [⁵¹Cr] release assays against freshly isolated tumor cells from patients with Waldenström disease (left panel) or CLL (right panel). PMNs served as effector cells at an E:T ratio of 80:1; antibody concentrations were 10 µg/mL. Results are mean ± SEM from ≥2 experiments with effector cells from different donors. *Significant difference specific antibody vs isotype control. †Significant difference RTX-IgA2 vs OBI-IgA2. #Significant difference IgG1 vs IgA2. Significant differences (*P* < .05) were calculated using ANOVA. ctrl., control; n.s., not significant; OBI, OBI-IgA2.

OBI-IgA2 is more effective than RTX-IgA2 or OFA-IgA2 in direct lymphoma cell killing

Next, we investigated direct cell death induction by CD20 antibodies of the IgG1 or IgA2 isotype, starting by visualizing homotypic aggregation of lymphoma cells, which has been described to correlate with the induction of direct cell death.³⁸ As IgG1, the type II antibody OBI induced the greatest degree of homotypic aggregation, followed by RTX and OFA (Figure 5A, upper panels). Interestingly, IgA2 variants of RTX and OFA also triggered homotypic cell aggregation to a similar degree as OBI-IgG1 and OBI-IgA2 (Figure 5A, lower panels). Using flow cytometric assessment of apoptosis induction by DioC6 staining, OBI as IgG1 and IgA2, but not the RTX or OFA isotype variants, induced significant direct cell death (Figure 5B). To further investigate the mechanism of cell death induction by CD20 antibodies of the IgA2 isotype, we investigated lysosomal cell death induction by LysoTracker Red staining.²¹ Again, OBI-IgG1 and OBI-IgA2 were most effective, but RTX-IgA2 also induced significant loss of lysosomal volume (Figure 5C). Next, we compared the capability of IgG1 and IgA2 variants of the 3 CD20 antibodies to form CD20-containing lipid rafts, a functional characteristic of type I antibodies. Interestingly, this activity of CD20 antibodies also remained unaffected by the isotype switch from IgG1 to IgA2, with both OBI variants

being significantly less effective than RTX or OFA variants (Figure 5D). We then investigated the mechanism of direct cell death induction by OBI-IgA2 in more detail using a pan-caspase inhibitor (Z-VAD-FMK) or LatB as an actin polymerization inhibitor. As shown for CD20 antibodies of the IgG1 isotype,²¹ apoptosis induction by OBI-IgA2 was independent of caspases (Figure 5E) but was fully dependent on actin polymerization (Figure 5F). Additionally, a V11L mutation in the constant region of the heavy chain, which was previously described to reduce lysosomal cell death induction by OBI-IgG1,³⁹ also impaired lysosomal cell death induction by OBI-IgA2 (Figure 5G) but did not negatively affect its ADCC capacity by PMNs (supplemental Figure 4A). Together, these data show that CD20-IgA antibodies trigger direct lymphoma cell killing similar to their IgG1 counterparts.

In vivo efficacy of IgA2 antibodies against CD20

We then investigated our novel IgA2 antibodies against CD20 in 3 in vivo models using human CD89-Tg mice. In an intraperitoneal tumor model, mice were injected with 5×10^6 human CD20-transduced EL4 (EL4-CD20) cells (Figure 6A). Twenty-four hours after monoclonal antibody injection, the remaining EL4-CD20 cells were quantified from peritoneal lavages by flow cytometry. OBI-IgA2, but not RTX-IgA2 or OFA-IgA2, significantly reduced the number of EL4-CD20 cells found in the peritoneal cavity (Figure 6B). Interestingly, all 3 IgA2

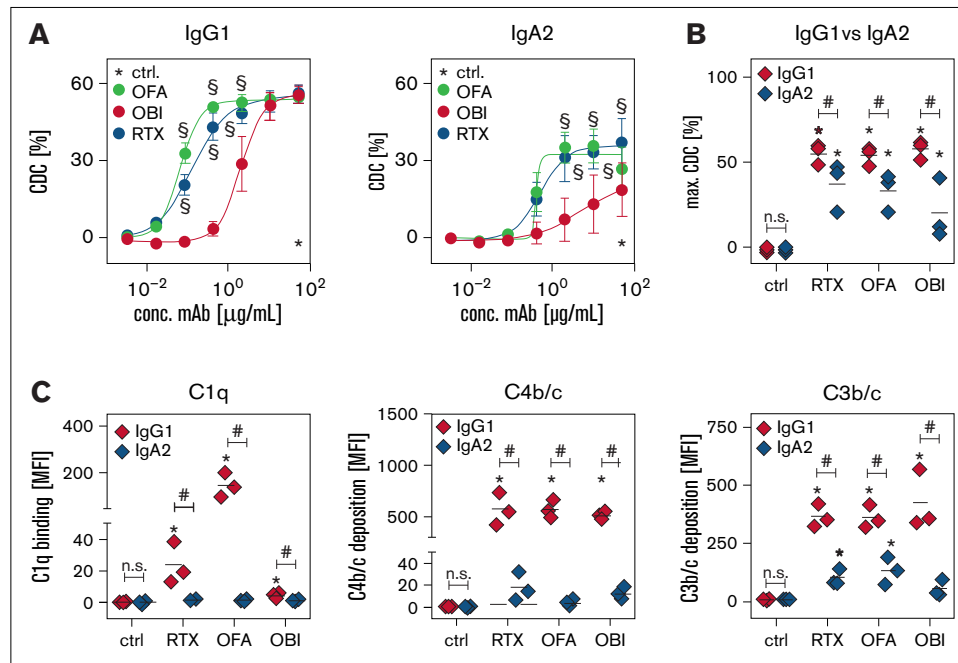


Figure 4. CD20 antibodies of the IgA isotype differ in their capacity to trigger CDC. (A) The CDC activity of CD20 antibodies of the IgG1 (left panel) or IgA2 (right panel) isotype was analyzed in [⁵¹Cr] release assays against SU-DHL-4 cells using increasing concentrations of antibodies. (B) Comparison of the maximal CDC activity of CD20-IgG1 and CD20-IgA2 antibodies, as determined in (A). (C) CD20 antibody-triggered binding (C1q) and deposition of complement components (C4b/c, C3b/c) on SU-DHL-4 cells was analyzed by indirect flow cytometry. CD20 antibodies were added at 10 $\mu\text{g/mL}$ for 60 minutes. Results are mean \pm SEM from ≥ 3 experiments. *Significant difference specific antibody vs isotype control. [§]Significant difference between OBI-IgA2 and RTX-IgA2 or OFA-IgA2. #Significant difference IgG1 vs IgA2. Significant differences ($P < .05$) were calculated using ANOVA. conc., concentration; ctrl, control; MFI, mean fluorescence intensity; n.s., not significant.

antibodies recruited neutrophils to the peritoneal cavity, with OBI-IgA2 causing the greatest neutrophil influx (Figure 6C).

In a second in vivo model, we investigated depletion of syngeneic human CD20-transgenic B cells by IgA2 antibodies (Figure 6D). In this experiment, all 3 CD20 IgA2 antibodies mediated significant B-cell depletion, with OBI-IgA2 causing more effective B-cell killing than RTX-IgA2 or OFA-IgA2 (Figure 6E). Next, we explored the relative importance of potential effector mechanisms of OBI-IgA2 in this model. Thus, we used an OBI-IgA2 variant (V11L) with a reduced capacity to induce lysosomal cell death but preserved ADCC function (see Figure 5G; supplemental Figure 4A), treated mice with cobra venom factor (CVF) to halt complement activation, or used CD89 nontransgenic (NTg) mice to lose the ADCC capacity of IgA antibodies. Interestingly, reduction in direct cell killing capacity, lack of complement activation, or a combination thereof did not have a significant effect on B-cell depletion by OBI-IgA2 in vivo. However, human CD89 expression was required for OBI-IgA2-mediated B-cell depletion, because B-cell depletion in CD89-NTg mice was significantly impaired compared with that in CD89-Tg mice (Figure 6F).

Additionally, we performed in vivo B-cell depletion experiments in human CD89/CD20 double-Tg mice (Figure 6G). Results showed that OBI-IgA2 achieved significant B-cell depletion compared with PBS treatment in CD89-Tg mice during and shortly after antibody injections, but B-cell numbers returned to normal over time (Figure 6H, middle panel). However, when CD89-NTg mice were used in these experiments, OBI-IgA did not significantly deplete B cells (Figure 6H, right panel), again indicating the importance of Fc α RI (CD89) and

effector cell-mediated tumor cell-killing mechanisms for OBI-IgA2's therapeutic efficacy in vivo.

In conclusion, our results indicate that investigations into antibodies' effector mechanisms can be essential for choosing the most appropriate CD20 antibody candidate for particular applications. For the recruitment of myeloid effector cells, and PMNs in particular, the variable regions of OBI proved more effective than did those of RTX or OFA. These observations may be particularly relevant in the therapeutic context of myeloid checkpoint blockade (eg, by CD47-blocking antibodies or by glutaminyl cyclase inhibitors).

Discussion

Here, we demonstrate that OBI-IgA2 was particularly effective in triggering myeloid cell-mediated killing of lymphoma cells in vitro and in vivo. This observation may become relevant in combination with myeloid checkpoint blocking therapy (eg, by magrolimab [Hu5F9-G4]⁴⁰ or by glutaminyl cyclase inhibitors²⁹) because myeloid cells, and PMNs in particular, are effectively activated by human IgA antibodies.

Studies into the mechanisms of action of clinically approved monoclonal antibodies hold promise to identify approaches to improve their therapeutic efficacy.⁵ In the context of CD20 antibodies, the second-generation antibody OFA is differentiated from RTX by its superior CDC activity.⁴¹ OBI as a third-generation antibody is the only approved type II CD20 antibody with enhanced programmed cell death (PCD) and reduced CDC activity compared with the type I antibodies RTX and OFA.³⁹ Additionally, OBI is produced as a low

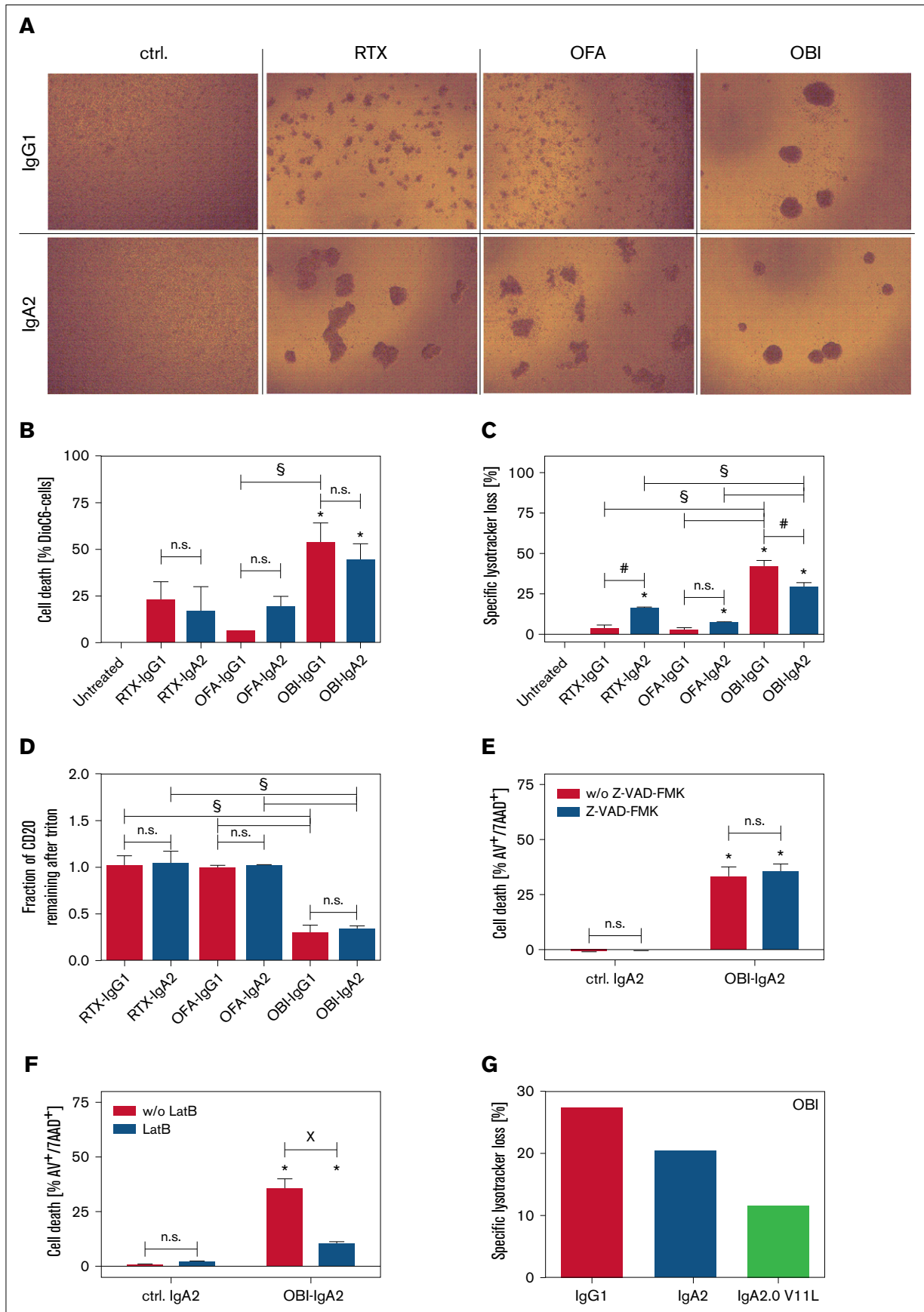


Figure 5.

fucosylated IgG1 antibody, which improves Fc γ R111 (CD16) binding and, thereby, enhances ADCC by NK cells.^{42,43} However, all 3 CD20 antibodies were not effective in triggering ADCC by PMNs and were similarly effective in recruiting macrophages for engulfment of target cells (Figure 1), with the latter being in agreement with previous observations.⁴⁴

Importantly, ADCP by macrophages, but not ADCC by PMNs, was enhanced in the presence of CD47 blockade. Because myeloid cells were demonstrated to critically contribute to CD20 antibody efficacy in mice,^{3,4} are the main recruited effector cell population resulting from myeloid checkpoint blockade with CD47 antibodies,^{6,8,9} and often are activated more effectively by IgA antibodies than by IgG1 antibodies,^{14,16,17} we evaluated the functional impact of switching the 3 approved CD20 antibodies from the human IgG1 isotype to the human IgA2 isotype.

The most unexpected finding is the observation that OBI-IgA2 was consistently more effective than RTX-IgA2 or OFA-IgA2 in triggering ADCC by PMNs. Although the underlying mechanisms of tumor cell killing by T or NK cells were intensively investigated and are quite well understood,⁴⁵ PMN-mediated tumor cell killing was only recently reported to depend on “trogoptosis,” a process that relates to trogocytosis leading to frustrated phagocytosis and, eventually, tumor cell death.⁴⁶ Macrophage-mediated tumor cell phagocytosis has been demonstrated to be enhanced when tumor-targeting antibodies bind to membrane-distal regions of target antigens, whereas NK cell-mediated ADCC and CDC are more effective when antibodies bind to epitopes that are closer to the tumor cell membrane.^{47,48} To our knowledge, results from similar studies are not available for PMNs but could not explain the differences among CD20 antibodies, which all bind to partially overlapping epitopes close to the cell membrane.

Tumor cell killing by PMNs was described to critically depend on target antigen density,⁴⁶ but other less well-defined target antigen characteristics were observed.^{27,47} The CD20 antigen is a member of the MSA4 protein family with 2 rather small extracellular loops,^{49,50} which predominantly forms double-barrel dimers.⁵⁰ The antigen binding sites for the 3 approved CD20 antibodies have been well defined and are partially overlapping.⁵¹⁻⁵³ The enhanced NK cell-mediated ADCC by OBI compared with RTX and OFA has been explained by OBI's low fucosylated Fc part, which is an established glycomodification used to improve Fc γ R111 binding for IgG antibodies.^{42,54} However, binding of IgA antibodies to Fc α RI (CD89) is not affected by antibodies' glycosylation³²; furthermore,

glycoprofiles of our 3 CD20 IgA antibodies were similar (supplemental Figure 2C). Together, these results suggest that an inherent feature of OBI's variable regions is particularly efficient in ADCC by PMNs. To analyze whether enhanced ADCC by PMNs is a general characteristic of type II CD20 antibodies of the IgA isotype, we generated and tested an IgA2 variant of the type II antibody 11B8. Interestingly, 11B8-IgA2 was also significantly more effective than RTX-IgA2 at triggering ADCC by PMNs (supplemental Figure 4B).

After intensive research by several groups, the fundamental differences between type I and type II CD20 antibodies have been related to differences in clustering of CD20 molecules by CD20 antibodies on the B-cell surface.^{51,53,55} Recent structural studies elegantly demonstrated that each CD20 dimer is bound by 2 RTX molecules, resulting in cross-linking of CD20 dimers into higher-order assemblies. In contrast to RTX, only 1 OBI molecule can bind to each CD20 dimer, thereby preventing more extensive CD20 cross-linking.^{51,53} Additional studies revealed that bivalent binding differed between CD20 antibodies: compared with OFA and RTX, OBI displayed the lowest amount of bivalent binding.⁵⁶ Furthermore, the elbow angle between VH and CH1 of OBI is wider compared with that of RTX, which is reversed by a V11L mutation in OBI.⁵⁷ Interestingly, V11L impaired direct lymphoma cell killing (Figure 5G) but did not negatively affect PMN-mediated ADCC (supplemental Figure 4A). Thus, type II antibodies of the IgA2 isotype are more effective than type I antibodies in triggering ADCC by PMNs, but their direct lymphoma killing capacity appears to be dispensable for enhanced ADCC by PMNs. In conclusion, differences in antibody orientation after antigen binding or in target antigen clustering on the lymphoma cell membrane appear to affect ADCC by PMNs.

To further improve neutrophil-mediated killing by CD20 antibodies, we explored the effects of CD47 blockade. Previous studies have demonstrated that RTX treatment benefits from blocking the CD47-SIRP α axis in preclinical models,⁴⁰ which appears to also translate into clinical benefit for lymphoma patients.¹¹ Macrophages were postulated to constitute the predominant effector cell type potentiated by this approach. Nevertheless, it is of interest to understand the impact of CD47 blockade on neutrophil-mediated killing.⁵⁸ Here, we show that, at least in vitro, IgG1 antibodies do not benefit from CD47 blockade in neutrophil-mediated ADCC. On the other hand, IgA2 antibodies showed significantly increased ADCP with macrophages and increased ADCC with neutrophils after CD47 blockade or glutaminyl cyclase inhibition, suggesting the promise of a combination therapy using IgA CD20 antibodies and myeloid checkpoint inhibition.

Figure 5. Direct lymphoma cell killing by CD20 antibodies of the IgA2 isotype. (A) Homotypic aggregation by CD20 antibodies was analyzed by phase-contrast microscopy using SU-DHL-4 target cells. Antibodies were added at 10 μ g/mL for 24 hours. Representative images of 3 independent experiments are shown. (B) Induction of direct cell death induced by CD20 monoclonal antibody was analyzed by DiOC6 staining. Ramos cells were used as target cells, and antibodies were added at a fixed concentration (10 μ g/mL) for 6 hours. (C) Lysosomal cell death was quantified by LysoTracker Red staining on Ramos cells after incubation with CD20 antibodies (10 μ g/mL) for 6 hours. (D) Redistribution of CD20 to lipid rafts was analyzed by flow cytometry on Ramos cells. For discrimination between nonraft and lipid raft distribution, cells were treated with Triton X-100 after incubation with 10 μ g/mL antibody for 6 hours. Residual fluorescence indicated Triton insolubility of formed lipid rafts. SU-DHL-4 cells were treated with the indicated CD20 antibodies at 10 μ g/mL for 24 hours in the presence of the pan caspase inhibitor Z-VAD-FMK (E) or the cytoskeleton inhibitor LatB (F). Subsequently, cells were stained with annexin V and 7-aminoactinomycin to assess cell death by flow cytometry. (F) Lysosomal cell death was quantified by LysoTracker Red staining on Ramos cells after incubation with CD20 antibodies (10 μ g/mL) for 6 hours. (G) Three OBI variants (IgG1, IgA2, and IgA2-V11L) were compared with regard to direct cell death induction. Lysosomal cell death was quantified by LysoTracker Red staining of Ramos cells after incubation with the antibodies (10 μ g/mL) for 6 hours. Results of 3 independent experiments are shown as mean \pm SEM, with the exception of (G), for which $n = 1$. *Significant difference specific antibody vs untreated/isotype control. #Significant difference IgG1 vs IgA2. ^xSignificant difference between with vs without inhibitor (Z-VAD-FMK or LatB). Significant differences ($P \leq .05$) were calculated using ANOVA. Original magnification $\times 20$ for panel A. AV, annexin V; ctrl., control; n.s., not significant; w/o, without; 7AAD, 7-aminoactinomycin.

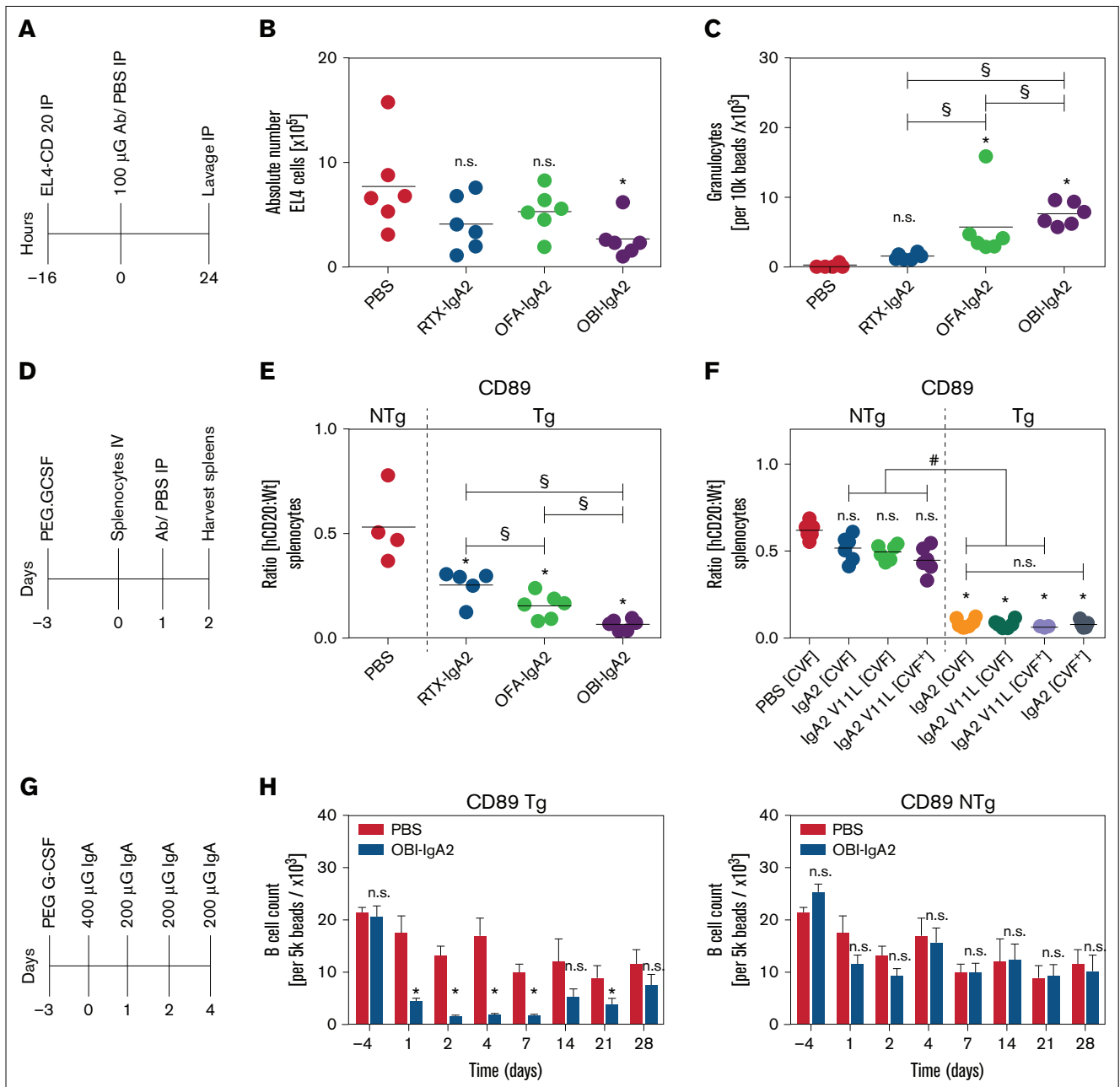


Figure 6. In vivo efficacy of IgA2 antibodies against CD20. (A) Schematic experimental overview of the short intraperitoneal (IP) model. (B) Absolute quantification of EL4-CD20 cells after intraperitoneal injection of the indicated CD20 IgA2 antibodies (100 µg per mouse). (C) Absolute quantification of intraperitoneal Ly6G⁺ granulocytes after treatment with the indicated CD20 IgA2 antibodies. (D) Schematic overview of the adoptive transfer model. (E) Ratio of labeled CD20-Tg/NTg splenic B cells after treatment of pegylated-granulocyte colony-stimulating factor-primed CD89-Tg or NTg mice with the indicated CD20 IgA2 antibodies (250 µg per mouse). (F) Ratio of labeled CD20-Tg/NTg B cells using CD89-Tg or NTg mice that did (CVF⁺) or did not (CVF⁻) receive intraperitoneal cobra venom factor (CVF) to deplete complement. Mice were treated with an unmodified (IgA2) or a PCD-impaired variant (IgA2 V11L) of OBI-IgA. (G) Schematic experimental overview of a syngeneic human CD20 Tg B-cell depletion model. (H) Quantification of remaining B cells after repeated treatment with OBI-IgA2, as indicated in (G), using CD89-Tg mice (left panel) or NTg mice (right panel). Results are presented as scatter dot blots (A-D) and as mean ± SEM of 6 mice per group (E). Statistical analyses were performed using 1-way ANOVA. *Significant difference vs PBS, unless indicated otherwise. #Significant difference OBI treatment NTg vs OBI treatment Tg. §Significant difference between different IgA2 antibodies. Horizontal line indicates the median. Ab, antibody; G-CSF, granulocyte colony-stimulating factor; h, human; n.s., not significant; Wt, wild-type.

In addition to ADCP and ADCC, we investigated complement activation by CD20 antibodies of the IgA2 isotype against lymphoma cell lines as another Fc-dependent effector mechanism. Although IgA antibodies lack a C1q binding site,³⁷ IgA antibodies against CD20

were reported to induce CDC in a C1q-dependent fashion.^{15,36,59} Similarly, other CD20 antibody molecules lacking a C1q binding site, such as IgG4 and F(ab')₂ fragments, showed activation of the classical complement pathway. Clustering of the B-cell receptor was

suggested as a potential mechanism for this so-called “bypass CDC,” which could then provide the required C1q binding moiety.⁵⁹ However, this explanation is controversial because the same type of complement activation was observed after knockout of the B-cell receptor,⁶⁰ suggesting that other molecules present within the CD20-containing lipid rafts may provide the required C1q binding site.

These previous results are confirmed by this study. As observed for IgG1 antibodies,⁶¹ IgA2 variants of the type I antibodies RTX and OFA were more effective in CDC induction compared with the type II antibody OBI. CDC has been demonstrated to contribute to the therapeutic efficacy of CD20 antibodies in particular mouse models²⁵ and may contribute to the induction of tumor-directed immune responses^{62,63}; however, its contribution to the clinical efficacy of CD20 antibodies has remained controversial.^{34,64,65} On the other hand, uncontrolled complement activation has been suggested to contribute to the first-dose toxicity of CD20 antibodies, which can be mediated by different mechanisms, including cytokine release.⁶⁶

Another suggested mechanism of action for CD20 antibodies is PCD induction, although its contribution to the clinical efficacy of CD20 antibodies is again controversial.⁶⁷ Previous studies have reported that an isotype switch of RTX from human IgG1 to IgG2 or IgG4 could affect PCD induction,⁶⁸ which was supposed to be related to differences in how these antibodies recognize CD20 tetramers on the lymphoma cell membrane.^{52,57} Within our panel of antibodies, IgG1 and IgA2 versions of the type II antibody OBI were the most effective in inducing direct cell death. As previously shown for OBI,^{21,69} PCD by OBI-IgA2 was also caspase independent but required a functional cytoskeleton. Interestingly, OBI-IgA2's PCD activity also appeared to depend on the antibody's elbow hinge region, because a V11L mutation reduced its PCD activity, as previously described for OBI-IgG1.³⁹ Conversion of type I CD20 antibodies from IgG1 to IgA2 unexpectedly increased homotypic aggregation, whereas lysosomal cell death and lipid raft induction remained mostly unchanged. Thus, overall direct effector mechanisms of the 3 CD20 antibodies were not affected by the isotype switch from IgG1 to IgA2. Importantly, PCD did not appear to contribute to B-cell depletion efficacy *in vivo*, because the OBI-IgA2 variant with reduced PCD activity *in vitro* (OBI-IgA2.0-V11L) was as effective as the OBI-IgA2 wild-type antibody *in vivo* (Figure 5F).

When we elucidated the mechanism of action of OBI-IgA2 *in vivo*, the presence of the human CD89 transgene proved essential for IgA's efficacy *in vivo* (Figure 6F). Together with results obtained after complement depletion by CVF or with the PCD-reduced OBI-IgA2-V11L variant, these observations demonstrated that Fc receptor-dependent mechanisms (ADCC or ADCP) were required, whereas PCD and CDC were dispensable for B-cell depletion by OBI-IgA2 *in vivo*. This dependency on CD89-dependent mechanisms could help to explain why OBI-IgA2 outperformed RTX-IgA2 and OFA-IgA2 in the same models, because the latter 2 were less effective in ADCC *in vitro*. Interestingly, OBI-IgA2 also was the most effective anti-CD20 IgA2 at recruiting PMNs into the peritoneal cavity (Figure 6C), the potential effector cell population in this model. Our results showing that IgA antibodies depend on Fc α RI (CD89) for *in vivo* efficacy are in line with results for other CD20 antibodies of the

IgA isotype^{15,36} and match with results for CD20 antibodies of the IgG1 isotype, which require activating Fc γ Rs for their therapeutic activity.^{3,70} Whether each of these monoclonal antibodies would be more effective in the IgG or IgA2.0 format requires further investigation using complex models encompassing all of the relevant Fc receptors and human target molecules.

Because myeloid checkpoint-blocking therapies (eg, CD47-blocking antibodies, such as magrolimab [Hu5F9-G4]) rely on ADCP or ADCC for their therapeutic efficacy, our results suggest that OBI may be a particularly promising CD20 antibody for this approach. An interesting observation within our *in vivo* B-cell depletion experiments was the decrease in B-cell numbers in the PBS control groups that were not treated with antibody, which was less pronounced than in OBI-IgA2-treated animals. We attribute these differences to the use of granulocyte colony-stimulating factor before the start of the experiment. Although granulocyte colony-stimulating factor was administered to improve granulocyte numbers and functions in the peripheral blood of mice, it was reported to suppress B lymphopoiesis.^{71,72}

We conclude that OBI-IgA2 is a CD20 antibody with exceptional B-cell killing properties *in vitro* and *in vivo*. In particular, OBI-IgA2's ability to recruit myeloid cells for ADCC and ADCP of lymphoma cells suggests that it could be an interesting molecule to combine with CD47-SIRP α -blocking strategies. Additional preclinical studies are required to assess the clinical potential of this approach.

Acknowledgments

This work was supported by German Research Organization grants DFG Pe 1425/5-1 (M.P.) and DFG Va 124/9-1 (T.V.), the Deutsche Krebshilfe “Mildred Scheel Professorship” program (M.P.), Dutch Cancer Research grant R3695 (M.E., M.J., and J.H.W.L.), Villa Joep grant 17 (M.N.), and grant 227 from the Dutch Kinderen Kankervrij Foundation (T.t.B.).

Authorship

Contribution: M.E., T.R., A.D., J.H.M.J., N.B., T.t.B., M.N., K.E., and K.R. performed experiments and analyzed data; M.E., T.R., J.H.W.L., and T.V. designed experiments and wrote the manuscript; J.H.W.L. and T.V. supervised the project; and all authors critically revised and reviewed the manuscript and approved the final version for submission.

Conflict-of-interest disclosure: J.H.W.L. is a cofounder of and shareholder in TigaTx. T.t.B. performed experiments at TigaTx, which also provided research funding to T.R. and T.V. The remaining authors declare no competing financial interests.

ORCID profiles: J.H.W.L., 0000-0003-4982-6914; T.V., 0000-0001-9181-8067.

Correspondence: Thomas Valerius, Section for Stem Cell Transplantation and Immunotherapy, Department of Medicine II, Christian Albrechts University and University Medical Center Schleswig-Holstein, Campus Kiel, Arnold Heller Str 3, D-24105 Kiel, Germany; e-mail: t.valerius@med2.uni-kiel.de.

References

1. Gentles AJ, Newman AM, Liu CL, et al. The prognostic landscape of genes and infiltrating immune cells across human cancers. *Nat Med*. 2015;21(8):938-945.
2. Sionov RV, Fridlender ZG, Granot Z. The multifaceted roles neutrophils play in the tumor microenvironment. *Cancer Microenviron*. 2015;8(3):125-158.
3. Uchida J, Hamaguchi Y, Oliver JA, et al. The innate mononuclear phagocyte network depletes B lymphocytes through Fc receptor-dependent mechanisms during anti-CD20 antibody immunotherapy. *J Exp Med*. 2004;199(12):1659-1669.
4. Gong Q, Ou Q, Ye S, et al. Importance of cellular microenvironment and circulatory dynamics in B cell immunotherapy. *J Immunol*. 2005;174(2):817-826.
5. Carter PJ, Lazar GA. Next generation antibody drugs: pursuit of the 'high-hanging fruit.' *Nat Rev Drug Discov*. 2018;17(3):197-223.
6. Feng M, Jiang W, Kim BYS, Zhang CC, Fu YX, Weissman IL. Phagocytosis checkpoints as new targets for cancer immunotherapy. *Nat Rev Cancer*. 2019;19(10):568-586.
7. Chao MP, Takimoto CH, Feng DD, et al. Therapeutic targeting of the macrophage immune checkpoint CD47 in myeloid malignancies. *Front Oncol*. 2020;9:1380.
8. Matlung HL, Szilagyi K, Barclay NA, van den Berg TK. The CD47-SIRP α signaling axis as an innate immune checkpoint in cancer. *Immunol Rev*. 2017;276(1):145-164.
9. Treffers LW, Ten Broeke T, Rösner T, et al. IgA-mediated killing of tumor cells by neutrophils is enhanced by CD47-SIRP α checkpoint inhibition. *Cancer Immunol Res*. 2020;8(1):120-130.
10. Chao MP, Alizadeh AA, Tang C, et al. Anti-CD47 antibody synergizes with rituximab to promote phagocytosis and eradicate non-Hodgkin lymphoma. *Cell*. 2010;142(5):699-713.
11. Advani R, Flinn I, Popplewell L, et al. CD47 blockade by Hu5F9-G4 and rituximab in non-Hodgkin's lymphoma. *N Engl J Med*. 2018;379(18):1711-1721.
12. Rösner T, Kahle S, Montenegro F, et al. Immune effector functions of human IgG2 antibodies against EGFR. *Mol Cancer Ther*. 2019;18(1):75-88.
13. Brandsma AM, Bondza S, Evers M, et al. Potent Fc receptor signaling by IgA leads to superior killing of cancer cells by neutrophils compared to IgG. *Front Immunol*. 2019;10:704.
14. Dechant M, Beyer T, Schneider-Merck T, et al. Effector mechanisms of recombinant IgA antibodies against epidermal growth factor receptor. *J Immunol*. 2007;179(5):2936-2943.
15. Lohse S, Loew S, Kretschmer A, et al. Effector mechanisms of IgA antibodies against CD20 include recruitment of myeloid cells for antibody-dependent cell-mediated cytotoxicity and complement-dependent cytotoxicity. *Br J Haematol*. 2018;181(3):413-417.
16. Dechant M, Vidarsson G, Stockmeyer B, et al. Chimeric IgA antibodies against HLA class II effectively trigger lymphoma cell killing. *Blood*. 2002;100(13):4574-4580.
17. Boross P, Lohse S, Nederend M, et al. IgA EGFR antibodies mediate tumour killing in vivo. *EMBO Mol Med*. 2013;5(8):1213-1226.
18. Otten MA, Rudolph E, Dechant M, et al. Immature neutrophils mediate tumor cell killing via IgA but not IgG Fc receptors. *J Immunol*. 2005;174(9):5472-5480.
19. Lohse S, Meyer S, Meulenbroek LA, et al. An anti-EGFR IgA that displays improved pharmacokinetics and myeloid effector cell engagement in vivo. *Cancer Res*. 2016;76(2):403-417.
20. van Tetering G, Evers M, Chan C, Stip M, Leusen J. Fc engineering strategies to advance IgA antibodies as therapeutic agents. *Antibodies (Basel)*. 2020;9(4):70.
21. Chan HT, Hughes D, French RR, et al. CD20-induced lymphoma cell death is independent of both caspases and its redistribution into Triton X-100 insoluble membrane rafts. *Cancer Res*. 2003;63(17):5480-5489.
22. Terszowski G, Klein C, Stern M. KIR/HLA interactions negatively affect rituximab- but not GA101 (obinutuzumab)-induced antibody-dependent cellular cytotoxicity. *J Immunol*. 2014;192(12):5618-5624.
23. Herter S, Birk MC, Klein C, Gerdes C, Umana P, Bacac M. Glycoengineering of therapeutic antibodies enhances monocyte/macrophage-mediated phagocytosis and cytotoxicity. *J Immunol*. 2014;192(5):2252-2260.
24. Wirt T, Roskopf S, Rösner T, et al. An Fc double-engineered CD20 antibody with enhanced ability to trigger complement-dependent cytotoxicity and antibody-dependent cell-mediated cytotoxicity. *Transfus Med Hemother*. 2017;44(5):292-300.
25. Di Gaetano N, Cittera E, Nota R, et al. Complement activation determines the therapeutic activity of rituximab in vivo. *J Immunol*. 2003;171(3):1581-1587.
26. Boross P, Jansen JH, de Haij S, et al. The in vivo mechanism of action of CD20 monoclonal antibodies depends on local tumor burden. *Haematologica*. 2011;96(12):1822-1830.
27. Derer S, Glorius P, Schlaeth M, et al. Increasing Fc γ RIIa affinity of an Fc γ RIII-optimized anti-EGFR antibody restores neutrophil-mediated cytotoxicity. *MAbs*. 2014;6(2):409-421.
28. Schewe DM, Alsadeq A, Sattler C, et al. An Fc-engineered CD19 antibody eradicates MRD in patient-derived MLL-rearranged acute lymphoblastic leukemia xenografts. *Blood*. 2017;130(13):1543-1552.

29. Logtenberg MEW, Jansen JHM, Raaben M, et al. Glutaminy cyclase is an enzymatic modifier of the CD47- SIRP α axis and a target for cancer immunotherapy. *Nat Med*. 2019;25(4):612-619.
30. Würflein D, Dechant M, Stockmeyer B, et al. Evaluating antibodies for their capacity to induce cell-mediated lysis of malignant B cells. *Cancer Res*. 1998;58(14):3051-3058.
31. Ferrara C, Stuart F, Sondermann P, Brünker P, Umaña P. The carbohydrate at Fc γ RIIIa Asn-162. An element required for high affinity binding to non-fucosylated IgG glycoforms. *J Biol Chem*. 2006;281(8):5032-5036.
32. Gomes MM, Wall SB, Takahashi K, Novak J, Renfrow MB, Herr AB. Analysis of IgA1 N-glycosylation and its contribution to Fc α RI binding. *Biochemistry*. 2008;47(43):11285-11299.
33. Golay J, Zaffaroni L, Vaccari T, et al. Biologic response of B lymphoma cells to anti-CD20 monoclonal antibody rituximab in vitro: CD55 and CD59 regulate complement-mediated cell lysis. *Blood*. 2000;95(12):3900-3908.
34. Kennedy AD, Beum PV, Solga MD, et al. Rituximab infusion promotes rapid complement depletion and acute CD20 loss in chronic lymphocytic leukemia. *J Immunol*. 2004;172(5):3280-3288.
35. Beers SA, Chan CH, James S, et al. Type II (tositumomab) anti-CD20 monoclonal antibody out performs type I (rituximab-like) reagents in B-cell depletion regardless of complement activation. *Blood*. 2008;112(10):4170-4177.
36. Pascal V, Laffleur B, Debin A, et al. Anti-CD20 IgA can protect mice against lymphoma development: evaluation of the direct impact of IgA and cytotoxic effector recruitment on CD20 target cells. *Haematologica*. 2012;97(11):1686-1694.
37. de Sousa-Pereira P, Woof JM. IgA: structure, function, and developability. *Antibodies (Basel)*. 2019;8(4):E57.
38. Ivanov A, Beers SA, Walshe CA, et al. Monoclonal antibodies directed to CD20 and HLA-DR can elicit homotypic adhesion followed by lysosome-mediated cell death in human lymphoma and leukemia cells. *J Clin Invest*. 2009;119(8):2143-2159.
39. Mössner E, Brünker P, Moser S, et al. Increasing the efficacy of CD20 antibody therapy through the engineering of a new type II anti-CD20 antibody with enhanced direct and immune effector cell-mediated B-cell cytotoxicity. *Blood*. 2010;115(22):4393-4402.
40. Liu J, Wang L, Zhao F, et al. Pre-clinical development of a humanized anti-CD47 antibody with anti-cancer therapeutic potential. *PLoS One*. 2015;10(9):e0137345.
41. Teeling JL, French RR, Cragg MS, et al. Characterization of new human CD20 monoclonal antibodies with potent cytolytic activity against non-Hodgkin lymphomas. *Blood*. 2004;104(6):1793-1800.
42. Herter S, Herting F, Mundigl O, et al. Preclinical activity of the type II CD20 antibody GA101 (obinutuzumab) compared with rituximab and ofatumumab in vitro and in xenograft models. *Mol Cancer Ther*. 2013;12(10):2031-2042.
43. Shields RL, Lai J, Keck R, et al. Lack of fucose on human IgG1 N-linked oligosaccharide improves binding to human Fc γ RIII and antibody-dependent cellular toxicity. *J Biol Chem*. 2002;277(30):26733-26740.
44. VanDerMeid KR, Elliott MR, Baran AM, Barr PM, Chu CC, Zent CS. Cellular cytotoxicity of next-generation CD20 monoclonal antibodies. *Cancer Immunol Res*. 2018;6(10):1150-1160.
45. Davis ZB, Vallera DA, Miller JS, Felices M. Natural killer cells unleashed: checkpoint receptor blockade and BiKE/TriKE utilization in NK-mediated anti-tumor immunotherapy. *Semin Immunol*. 2017;31:64-75.
46. Matlung HL, Babes L, Zhao XW, et al. Neutrophils kill antibody-opsonized cancer cells by trogoptosis. *Cell Rep*. 2018;23(13):3946-3959.e6.
47. Cleary KLS, Chan HTC, James S, Glennie MJ, Cragg MS. Antibody distance from the cell membrane regulates antibody effector mechanisms. *J Immunol*. 2017;198(10):3999-4011.
48. Li J, Stagg NJ, Johnston J, et al. Membrane-proximal epitope facilitates efficient T cell synapse formation by anti-FcRH5/CD3 and is a requirement for myeloma cell killing. *Cancer Cell*. 2017;31(3):383-395.
49. Tedder TF, Streuli M, Schlossman SF, Saito H. Isolation and structure of a cDNA encoding the B1 (CD20) cell-surface antigen of human B lymphocytes. *Proc Natl Acad Sci USA*. 1988;85(1):208-212.
50. Eon Kuek L, Leffler M, Mackay GA, Hulett MD. The MS4A family: counting past 1, 2 and 3. *Immunol Cell Biol*. 2016;94(1):11-23.
51. Rougé L, Chiang N, Steffek M, et al. Structure of CD20 in complex with the therapeutic monoclonal antibody rituximab. *Science*. 2020;367(6483):1224-1230.
52. Klein C, Lammens A, Schäfer W, et al. Epitope interactions of monoclonal antibodies targeting CD20 and their relationship to functional properties. *MAbs*. 2013;5(1):22-33.
53. Kumar A, Planchais C, Fronzes R, Mouquet H, Reyes N. Binding mechanisms of therapeutic antibodies to human CD20. *Science*. 2020;369(6505):793-799.
54. Valgardsdottir R, Cattaneo I, Klein C, Introna M, Figliuzzi M, Golay J. Human neutrophils mediate trogocytosis rather than phagocytosis of CLL B cells opsonized with anti-CD20 antibodies. *Blood*. 2017;129(19):2636-2644.
55. Sopp J, Cragg MS. Deleting malignant B cells with second-generation anti-CD20 antibodies. *J Clin Oncol*. 2018;36(22):2323-2325.
56. Bondza S, Ten Broeke T, Nestor M, Leusen JHW, Buijs J. Bivalent binding on cells varies between anti-CD20 antibodies and is dose-dependent. *MAbs*. 2020;12(1):1792673.
57. Niederfellner G, Lammens A, Mundigl O, et al. Epitope characterization and crystal structure of GA101 provide insights into the molecular basis for type I/II distinction of CD20 antibodies. *Blood*. 2011;118(2):358-367.
58. Valerius T, Rösner T, Leusen JHW. CD47 blockade and rituximab in non-Hodgkin's lymphoma. *N Engl J Med*. 2019;380(5):496-497.

59. Engelberts PJ, Voorhorst M, Schuurman J, et al. Type I CD20 antibodies recruit the B cell receptor for complement-dependent lysis of malignant B cells. *J Immunol*. 2016;197(12):4829-4837.
60. Evers M, Kruse E, Hamdan F, Lebbink RJ, Leusen JHW. Comment on "Type I CD20 antibodies recruit the B cell receptor for complement-dependent lysis of malignant B cells". *J Immunol*. 2018;200(8):2515-2516.
61. Marshall MJE, Stopforth RJ, Cragg MS. Therapeutic antibodies: what have we learnt from targeting CD20 and where are we going? *Front Immunol*. 2017;8:1245.
62. Zent CS, Pinney JJ, Chu CC, Elliott MR. Complement activation in the treatment of B-cell malignancies. *Antibodies (Basel)*. 2020;9(4):68.
63. Golay J, Taylor RP. The role of complement in the mechanism of action of therapeutic anti-cancer mAbs. *Antibodies (Basel)*. 2020;9(4):58.
64. Middleton O, Cosimo E, Dobbin E, et al. Complement deficiencies limit CD20 monoclonal antibody treatment efficacy in CLL. *Leukemia*. 2015;29(1):107-114.
65. Beurskens FJ, Lindorfer MA, Farooqui M, et al. Exhaustion of cytotoxic effector systems may limit monoclonal antibody-based immunotherapy in cancer patients. *J Immunol*. 2012;188(7):3532-3541.
66. Paul F, Cartron G. Infusion-related reactions to rituximab: frequency, mechanisms and predictors. *Expert Rev Clin Immunol*. 2019;15(4):383-389.
67. van Oers MH. CD20 antibodies: type II to tango? *Blood*. 2012;119(22):5061-5063.
68. Könitzer JD, Sieron A, Wacker A, Enenkel B. Reformating rituximab into human IgG2 and IgG4 isotypes dramatically improves apoptosis induction in vitro. *PLoS One*. 2015;10(12):e0145633.
69. Honeychurch J, Alduaij W, Azizyan M, et al. Antibody-induced nonapoptotic cell death in human lymphoma and leukemia cells is mediated through a novel reactive oxygen species-dependent pathway. *Blood*. 2012;119(15):3523-3533.
70. Clynes RA, Towers TL, Presta LG, Ravetch JV. Inhibitory Fc receptors modulate in vivo cytotoxicity against tumor targets. *Nat Med*. 2000;6(4):443-446.
71. Day RB, Bhattacharya D, Nagasawa T, Link DC. Granulocyte colony-stimulating factor reprograms bone marrow stromal cells to actively suppress B lymphopoiesis in mice. *Blood*. 2015;125(20):3114-3117.
72. Winkler IG, Bendall LJ, Forristal CE, et al. B-lymphopoiesis is stopped by mobilizing doses of G-CSF and is rescued by overexpression of the anti-apoptotic protein Bcl2. *Haematologica*. 2013;98(3):325-333.